Laminar Heat and Fluid Flow Characteristic with a Modified Temperature-Dependent Viscosity Model in a Rectangular Duct

Chang-Hyun Sohn*
School of Mechanical Engineering, Kyungpook National University, Daegu 702-701, Korea
Jae-Whan Chang
Korea Powertrain Co., 597-10, Daechun Dong, Dalseo Gu, Daegu 704-801, Korea

The present study proposes a modified temperature-dependent non-Newtonian viscosity model and investigates the flow characteristics and heat transfer enhancement of the viscoelastic non-Newtonian fluid in a 2:1 rectangular duct. The combined effects of temperature dependent viscosity, buoyancy, and secondary flow caused by the second normal stress difference are considered. Calculated Nusselt numbers by the modified temperature-dependent viscosity model give good agreement with the experimental results. The heat transfer enhancement of viscoelastic fluid in a rectangular duct is highly dependent on the secondary flow caused by the magnitude of second normal stress difference.

Key Words : Viscoelastic Fluid, Non-Newtonian Fluid, Non-Newtonian Viscosity Model, Temperature-Dependent Viscosity Model, Second Normal Stress Difference

Nomenclature

$\bar{D}_h$: Hydraulic diameter, m
Gr^*: Grashof number, $(\bar{g}\bar{\beta}\bar{q}''\bar{D}_h^3)/(\bar{k}_{ref}\bar{\eta}_{o,ref}^2)$
Gz : Graetz number, $(\bar{x}/\mathrm{Pr}\,\mathrm{Re}\,\bar{D}_h)^{-1}$
h : Heat transfer coefficient : W/(m·K)
k : Non-dimensional thermal conductivity of fluid, $\bar{k}/\bar{k}_{ref}$
n : Power law index
Nu : Nusselt number, $\bar{h}\bar{D}_h/\bar{k}=\bar{q}''\bar{D}_h/\bar{k}/(\bar{T}_{wall}-\bar{T}_{bulk})$
P : Non-dimensional pressure, $(\bar{P}-\bar{P}_{ref})/(\bar{\rho}_{ref}\bar{U}_{ref}^2)$
Q : A constant accounting for the temperature dependence of viscosity equation (5)
Pr^+ : Generalized Prandtl number, $\frac{K\bar{c}_{p,ref}}{\bar{k}_{ref}}\left(\frac{\bar{D}_h}{\bar{U}_{avg}}\right)^{1-n}$
$\bar{q}''$: Heat flux, W/m^2
Ra : Rayleigh number for constant heat flux boundary condition, $Gr^*\mathrm{Pr}$
Re : Reynolds number, $\bar{\rho}_{ref}\bar{D}_h\bar{U}_{ava}/K$
Re^+ : Generalized Reynolds number, $(\bar{\rho}_{ref}\bar{D}_h\bar{U}_{avg}^{2-n})/K$
T : Non-dimensional temperature, $(\bar{T}-\bar{T}_i)/(\bar{q}''\bar{D}_h/\bar{k}_{ref})$
u : Non-dimensional axial velocity
x : Non-dimensional axial distance, $\bar{x}/\bar{D}_h$
α_1 : First normal stress difference coefficient, $(\tau_{xx}-\tau_{yy})/\dot{\gamma}^2$
α_2 : Second normal stress difference coefficient, $(\tau_{yy}-\tau_{zz})/\dot{\gamma}^2$
$\dot{\gamma}$: Non-dimensional shear rate
η : Non-dimensional viscosity, $(\bar{U}_{avg}^{1-n}\bar{\eta})/(K\bar{D}_h^{1-n})$
τ : Stress

* Corresponding Author,
E-mail : chsohn@knu.ac.kr
TEL : +82-53-950-5570; **FAX** : +82-53-950-6550
School of Mechanical Engineering, Kyungpook National University Daegu 702-701, Korea. (Manuscript **Received** January 14, 2005; **Revised** February 2, 2006)

θ : Dimensionless temperature
δ_{ij} : Kronecker delta
$\_$: Dimensional state
ref : Reference state (at inlet temperature of 20℃)

1. Introduction

The understanding of the fluid dynamic and heat transfer behavior of non-Newtonian viscoelastic fluids in laminar flow through rectangular ducts is important because of the wide application of such geometries. Hartnett and his coworkers (1985; 1991; 1996) showed significant laminar heat transfer enhancements (up to 300%) with viscoelastic fluids in rectangular ducts, which had never been observed in a circular pipe flow. Several researchers have investigated the enhancement mechanism with experimental and numerical studies.

Hartnett and Kostic (1985) and Gao and Hartnett (1996) investigated the effect of secondary flows on non-Newtonian viscoelastic fluids in relation to fully-developed laminar heat transfer behavior in a rectangular duct. They used the Reiner-Rivlin constitutive equation with finite values for the second normal stress coefficient, and demonstrated that the significant enhancement in heat transfer was caused by a secondary flow.

Shin and Cho (1994) focused on temperature-dependent fluid viscosity as the reason for the heat transfer enhancement of non-Newtonian fluids in a rectangular duct. They recorded 70~200% heat transfer enhancements with polyacrylamide (Separan AP-273) in contrast to a constant-property flow. Chang et al.(1998) considered both temperature-dependent shear thinning viscosity and buoyancy-induced secondary flow; however, the resulting values of their Nusselt numbers were smaller than previous experimental results (Gao and Hartnett, 1996) in a fully-developed region with a polyacrylamide solution (Separan AP-273).

In recent years Shin et al.(1999) and Sohn et al.(2000) conducted a computational study that considered the effect of both temperature-dependent and a normal stress-induced secondary flow in an upper-wall-heated 2:1 aspect ratio rectangular duct that suppressed free convection. They reported that the values of the local Nusselt numbers calculated for a polyacrylamide solution were consistent with experimental results in both the thermally developing and developed regions.

However, the existing temperature-dependent viscosity model has a drawback of yielding a non-physical phenomenon that in which viscosity nearly approaches zero as temperature and shear rate increase. Hence, the objective of the present paper is to propose a modified temperature-dependent non-Newtonian viscosity model and investigate heat and mass transfer characteristics in a 2:1 rectangular duct for validating the proposed modified model.

2. Mathematical Formulation

2.1 Governing equations

Figure 1 shows a schematic diagram of the system for bottom wall heated case. Fluid enters the duct with a fully developed parabolic velocity profile and uniform temperature T_i. The heating conditions considered in the present study follows those in Hartnett and Kostic (1985) : a) bottom wall heated and b) both upper and bottom wall

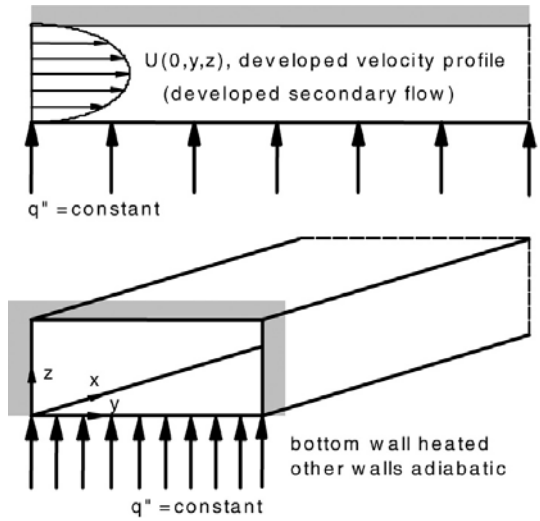

Fig. 1 Physical configurations of 2:1 rectangular duct with hydraulic and thermal boundary conditions for bottom wall heated case

heated with adiabatic boundary condition at the side walls.

A Boussinesq approximation was applied to consider the buoyancy effect whereas the viscous dissipation was neglected. The dimensionless governing equations for a steady three-dimensional laminar flow of an incompressible fluid can be expressed as follows :

Continuity

$$\frac{\partial u_i}{\partial x_i}=0 \tag{1}$$

Momentum

$$\frac{\partial(u_iu_j)}{\partial x_j}=-\frac{\partial P}{\partial x_i}+\frac{1}{\mathrm{Re}^+}\left(\frac{\partial \tau_{ij}}{\partial x_j}\right)+\delta_{3i}\frac{Gr^*}{(\mathrm{Re}^+)^2}T \tag{2}$$

Energy

$$\frac{\partial(Tu_j)}{\partial x_j}=\frac{1}{\mathrm{Pr}^+\mathrm{Re}^+}\left[\frac{\partial}{\partial x_j}\left(\frac{\partial T}{\partial x_j}\right)\right] \tag{3}$$

where Grashof number ($Gr^*=\mathrm{Ra}/\mathrm{Pr}$) is calculated by given experimental test conditions of Rayleigh number Ra, and Prandtl number.

A no-slip boundary condition was applied along the periphery of the duct for the velocity components and $\partial(u,v,w)/\partial x=0$ and $\partial^2T/\partial x^2=0$ were applied at the outlet.

The QUICK scheme by Hayase, Humphrey and Greif (1992) was employed in the discretization procedures for the convection terms of the governing equations. The convergence criterion was set up as $|\phi^{(n)step}-\phi^{(n-1)step}|\leq 10^{-7}$. Numerical experiments were conducted to determine an adequate grid number with a Newtonian fluid in a 2:1 duct. A 41×41 uniform grid at the cross section of the duct was chosen because the calculated results became independent of the number of grid points beyond a grid size of 41×41 (Ref. Kim et al., 1997).

2.2 Temperature-dependent viscosity models

Shi and Cho (1994) used the following temperature-dependent Carreau model as the shear-thinning temperature-dependent viscosity of a non-Newtonian fluid.

$$\frac{\eta(\gamma,\ T)-\eta_\infty}{\eta_{o,ref}10^{(\xi T)}-\eta_\infty}=[1+(De10^{(\xi T)}\gamma)^2]^{(n-1)/2} \tag{4}$$

where De is the Deborah number ($\lambda U_{avg}/D_h$), ξ is a constant accounting for the temperature dependence of the time constant (λ), and ζ represents the slope of the η_o verse T curve, and n is power law index. $\xi=-14.9$ and $\zeta=-8.35$ are given for Separan Ap-273 fluid.

There is no experimental η_∞ value in the Shin's data, but η_∞ is non-zero value at high shear rate and it becomes an asymptotic value as reported in many references (Xie and Hartnett, 1992 ; Rohsenow et al., 1998 ; Kostic, 1994).

Chang et al.(1998) used the non-Newtonian temperature-dependent viscosity model as follows.

$$n=\exp(-Q\theta)\,[\eta_\infty+(\eta_0-\eta_\infty)\{1+(Cu\dot\gamma)^2\}^{(n-1)/2}] \tag{5}$$

where Cu is a Carreau number ($Cu=De10^{(\xi T)}$), θ is the dimensionless temperature, $Q=b(\bar q''\bar D_h/\bar k_{ref})$ is a measure of magnitude of the temperature dependence for viscosity and $b=0.019$ is used.

Note that in viscosity models given by equation (4) and (5) the viscosity becomes zero as temperature increases.

In the present study we propose the modified temperature-dependent viscosity model as follows.

$$\eta=\exp(-Q\theta)\,[(\eta_0-\eta_\infty)\{1+(Cu\dot\gamma)^2\}^{(n-1)/2}]+\eta_\infty \tag{6}$$

where η_∞ is the low limiting viscosity and its value is obtained from Hartnett's experimental data (Xie and Hartnett, 1992) as $\eta_\infty=0.00015$.

Figure 2 shows a comparison of different viscosity models with experimental results (Shin and Cho, 1994). The Shin's viscosity model shown in Fig. 2(a) is crossing the curves at other temperatures. The Chang's viscosity model shown in Fig. 2(b) gives reasonably good agreement. However, in the above viscosity models, as shear rate and temperature increase, the viscosity approaches zero even though η_∞ is given a non-zero value. Figure 2(c) shows the results of the modified viscosity model. It is seen that the limiting viscosity approaches η_∞ as shear rate and temperature increase.

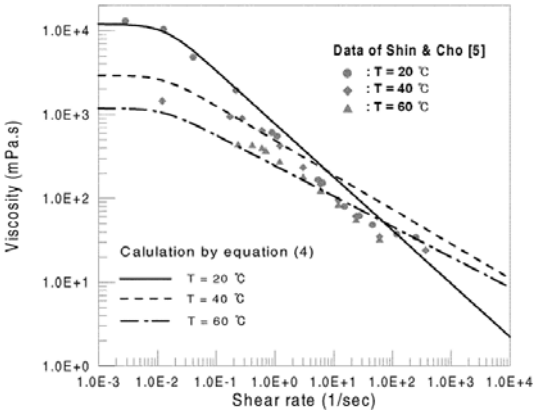

(a) Shin's model

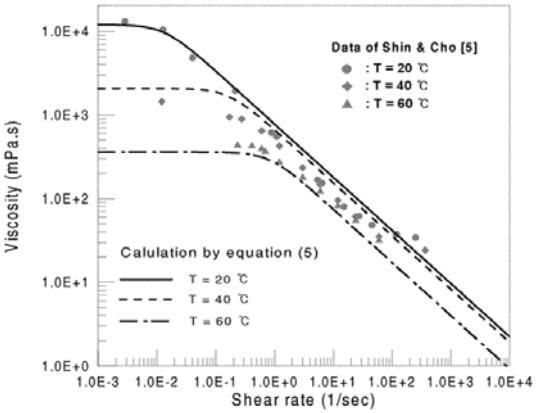

(b) Chang's model

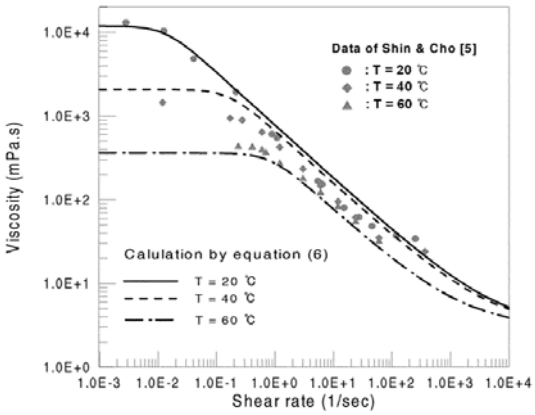

(c) Modified model

Fig. 2 The comparison of three viscosity models with experimental data

2.3 Reiner-Rivlin constitutive equation

Non-Newtonian viscoelastic fluids exhibit a normal stress difference under shear flow conditions. Green and Rivlin (1956) demonstrated the existence of a secondary flow in an elliptical duct flow using the following Reiner-Rivlin constitutive equation.

$$\tau_{ij}=\eta\dot{\gamma}_{ij}+\alpha_2\dot{\gamma}_{ik}\gamma_{kj} \tag{7}$$

where

$$\dot{\gamma}_{ij}=\left(\frac{\partial u_i}{\partial x_j}+\frac{\partial u_j}{\partial x_i}\right)$$
$$\alpha_2=(\mathrm{Re}^{+}/\bar{D}_h\bar{\rho}_{ref})\,\bar{\alpha}_2 \tag{8}$$

Gao and Hartnett (1996) applied the Reiner-Rivlin constitutive equation using values of α_2 ranging from 0.003 to 0.01 ($0.1\alpha_1\leq\alpha_2\leq0.3\alpha_1$), and they obtained heat transfer enhancement results which were consistent with the experimental results reported by Xie and Hartnett (1992). We compared calculated secondary velocity with the LDV measured secondary velocity given by Gervang and Larsen (1991), using various α_2 to obtain a correct second normal stress difference coefficient (α_2). Figure 3 shows the correct value of α_2 is about 0.15 times of first normal stress difference coefficient (α_1). However, Shin et al. (1999 : 2000) have used the values of $\alpha_2=0.1\alpha_1$.

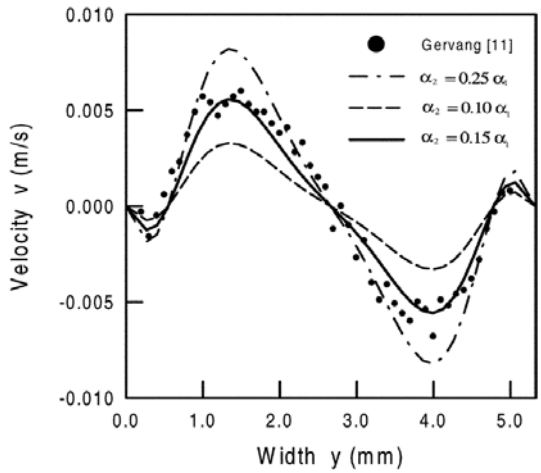

Fig. 3 Comparison of measured and calculated velocity profile $v(y)$

3. Results and Discussion

3.1 Flow characteristics

The secondary flow patterns for the case of heated bottom wall are shown in Fig. 4. Since

the circulating direction of the buoyancy-induced secondary flow was in the same direction as the lower cell of the viscoelastic-driven secondary flow, the secondary flow near the bottom wall increased in strength and expanded the circulation region. However, the secondary flow near the upper region circulated in the opposite direction to the buoyancy-induced secondary flow ; therefore, the strength and field of the upper secondary flow was reduced. As the flow progressed downstream, the secondary flow became a large single cell in a half cross section as shown in Fig. 4(c).

The secondary flows for both top and bottom heated wall case are shown in Fig. 5. Due to heating, the viscosity near the top wall decrease leading to increase in velocity and strength of secondary flow there. However, the secondary flow near bottom wall is seen to dominate in strength. Therefore, the strength and field of the upper secondary flow gradually reduced.

Figure 6 shows the calculated non-dimensional axial velocity profiles for the Separan solution along the vertical direction with different viscosity model. Note that $z=0$ refers to the heated bottom wall, $z=0.5$ refers to the unheated top wall (Fig. 1), and the velocity profile at $x=0.0$ represents the fully developed velocity profile for the constant-property fluid (CPF). Figure 6(a) shows that the maximum axial velocity at the mid-plane (i.e., at $y=0.5$) decreased compared to

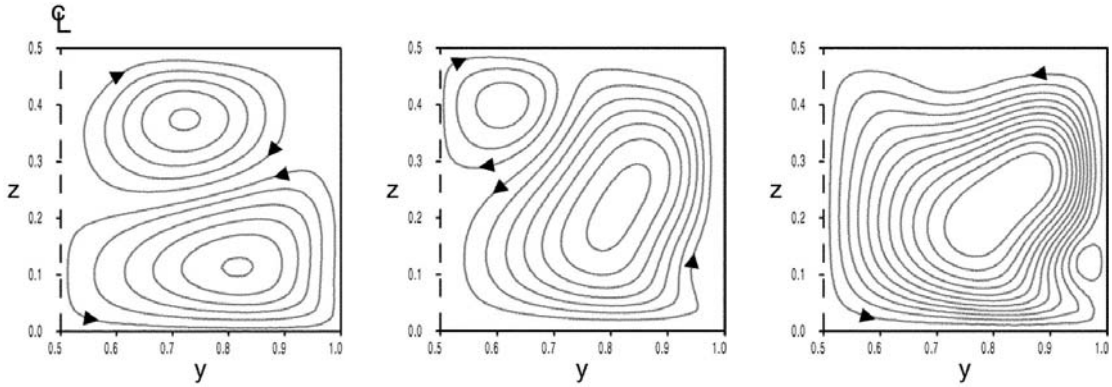

(a) $x=0.003$ (b) $x=0.01$ (c) $x=0.02$

Fig. 4 Development of secondary flow pattern along the dimensionless axial direction of case 1 (heated bottom wall)

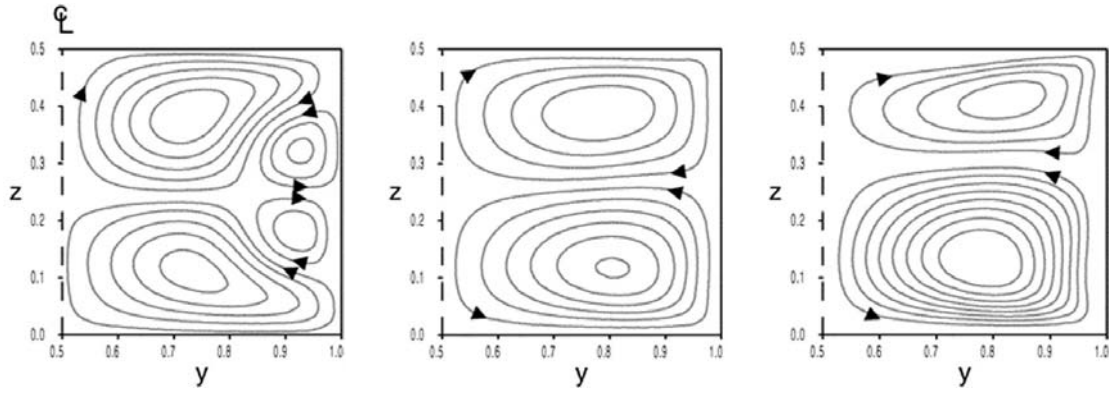

(a) $x=0.003$ (b) $x=0.01$ (c) $x=0.02$

Fig. 5 Development of secondary flow pattern along the dimensionless axial direction of case 2 (heated top and bottom wall)

that for CPF along the axial distance, whereas the maximum axial velocity near the side wall (i.e., at $y=0.1$) increased, see Fig. 6(b). Also, at $x=0.02$, the location of the maximum velocity is shifted from the center (i.e., $z=0.25$) of the rectangular duct compared to that at the inlet near the heated bottom wall. However the variation in the velocity profiles with Shin's viscosity model is larger than that with the present modified viscosity model. Hartnett and Kostic (1985) carried out careful pressure drop measurements of Separan solution and concluded that the influence of elasticity on pressure drop of a viscoelastic fluid is small and that, in general, the viscoelastic fluid behaves as a purely viscous non-Newtonian fluid. However Shin's viscosity model gives a lower viscosity at high temperature and a high shear rate and subsequently very large velocity variation and induce large pressure drop. The velocity profiles observed with the present model are consistent with the results of Hartnett and Kostic (1985).

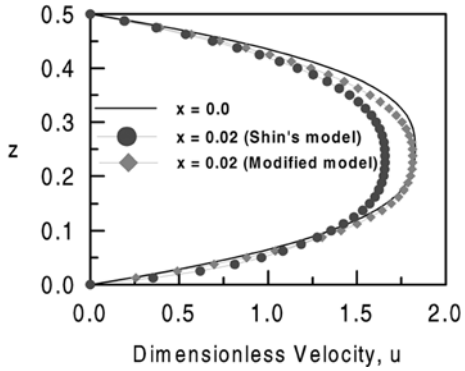

(a) $y=0.5$ (mid-plane)

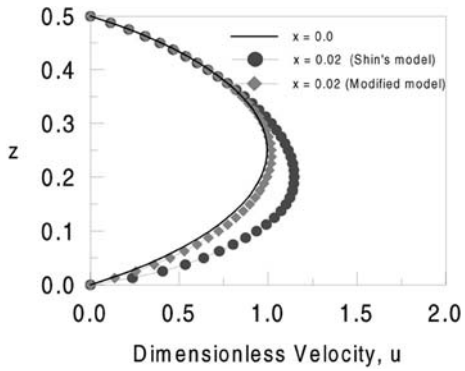

(b) $y=0.1$ (plane near the side wall)

Fig. 6 The comparison of two numerical results in 2:1 rectangular duct with bottom-wall heated

3.2 Heat transfer characteristics

Figures 7 and 8 show dimensionless temperature profiles calculated for CPF and Separan at $x=0.02$, respectively. The temperature near the heated bottom wall for CPF was much higher than that of Separan solution. For example, the temperature at the center of the bottom wall for CPF was 0.197 whereas that for Separan solution was 0.091. However, the temperature at the corner of top wall was much lower then Separan solution. The temperature profile for the Separan solution shown in Fig. 8 is much more complex than that of CPF. This is mainly due to the distortion of the flow associated with the combined secondary flow caused by the second normal stress difference and buoyancy effect. The minimum temperature seen at $y=0.5$ is consistent with the secondary flow region seen in Fig. 4.

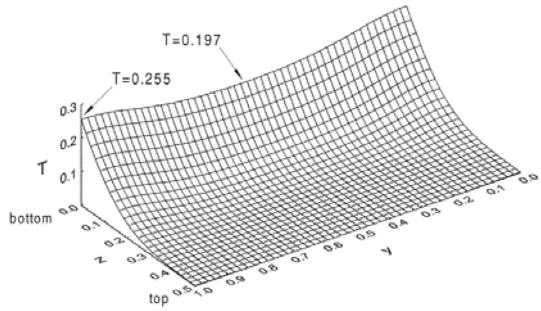

Fig. 7 Dimensionless cross-sectional temperature profile at $x=0.02$ of CPF (heated bottom wall)

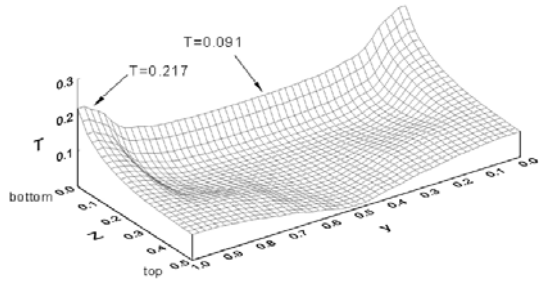

Fig. 8 Dimensionless cross-sectional temperature profile at $x=0.02$ of Separan (heated bottom wall)

In order to examine the heat transfer enhancement by the different temperature-dependent viscosity models on the laminar heat transfer for Separan solution, local Nusselt numbers for CPF and Separan are shown in Figs. 9 and 10. The heat transfer experiments (Xie and Hartnett, 1982) were carried out with Re=511.3, Pr=54.40 and 10^{-5}Ra= 0.89 for bottom wall heated case (Fig. 9) and the corresponding values of $\bar{q}''$ is 1.217. The experimental conditions of Fig. 10 for both top and bottom wall heated case were Re=433.3, Pr=63.7, 10^{-5}Ra=0.69, and the obtained value of $\bar{q}''$ is 1.104.

In the thermally-fully-developed region, the present calculation for CPF yield a Nusselt number of 3.56, which is almost identical to the analytical value of 3.54. Nusselt number of modified viscosity model is slightly lower than that of the other viscosity models since the calculations were carried out with the lowest α_2 value ($\alpha_2=0.1\alpha_1$) in Reiner-Rivlin constitutive equation.

However, the calculated local Nusselt numbers with the correct value of the second normal stress difference coefficient ($\alpha_2=0.15\alpha_1$) gives very good results as shown in Figs. 11 and 12. When an attempt was made to incorporated $\alpha_2=0.15\alpha_1$ in the other models, the agreement with the experiments was very poor and the results show the existing temperature-dependent viscosity models exaggerate the effect of temperature-dependent viscosity on the laminar heat transfer enhancement with a very low viscosity in the regions of

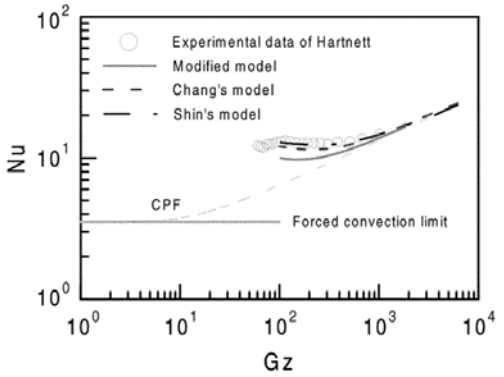

Fig. 9 The comparison of three numerical results with $\alpha_2=0.1\alpha_1$ in 2:1 rectangular duct with bottom-wall heated

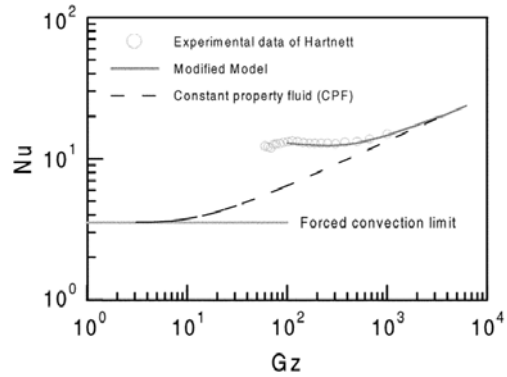

Fig. 11 The comparison of two numerical results with $\alpha_2=0.15\alpha_1$ in 2:1 rectangular duct with bottom wall heated

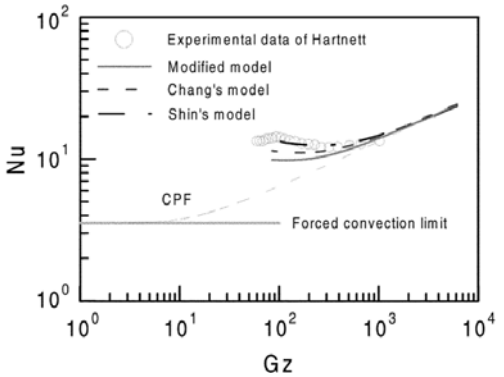

Fig. 10 The comparison of three numerical results with $\alpha_2=0.1\alpha_1$ in 2 :1 rectangular duct with top & bottom-wall heated

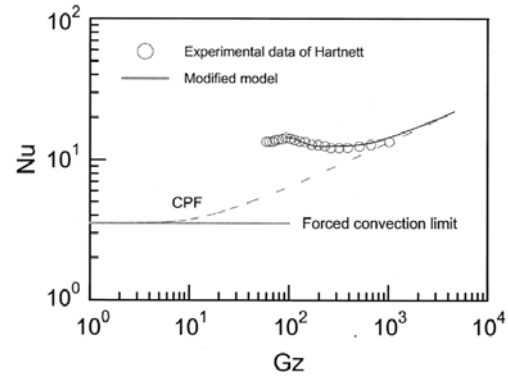

Fig. 12 The comparison of two numerical results with $\alpha_2=0.15\alpha_1$ in 2:1 rectangular duct with top & bottom wall heated

high temperature and shear rate.

4. Conclusions

The present numerical study examined existing temperature-dependent viscosity models and a modified temperature-dependent viscosity model on the laminar heat transfer behavior in a 2:1 rectangular duct. The key findings are as follows :

(1) The proposed temperature-dependent viscosity model predicts the limiting viscosity tending to η_∞, even though both shear rate and temperature increase.

(2) A correct second normal stress difference coefficient is about 0.15 times of first normal stress difference coefficient.

(3) The calculated local Nusselt numbers using the modified temperature-dependent viscosity model with the correct value of $\alpha_2(=0.15\alpha_1)$ are consistent with experimental results.

(4) The existing temperature-dependent viscosity models exaggerate the effect of temperature-dependent viscosity on the laminar heat transfer enhancement in a 2:1 rectangular duct with a very low viscosity in the regions of high temperature and shear rate.

(5) The main cause of the heat transfer enhancement of the Separan solution is viscoelastic-driven secondary flow, with buoyancy and variable viscosity in supporting roles.

Acknowledgments

This work has been funded by Brain Korea 21 project.

References

Chang, P. Y., Chou, F. C. and Tung, C. W., 1998, "Heat Transfer Mechanism for Newtonian and Non-Newtonian Fluids in 2:1 Rectangular Ducts," *International Journal of Heat and Mass Transfer*, Vol. 41, pp. 3841～3856.

Gao, S. X. and Hartnett, J. P., 1996, "Heat Transfer behavior of Reiner-Rivlin Fluids in Rectangular Ducts," *International Journal of Heat and Mass Transfer*, Vol. 39, pp. 1317～1324.

Gervang, B. and Larsen, P. S., 1991, "Secondary Flows in Straight Ducts of Rectangular Cross Section," *J. Non-Newtonian Fluid Mechanics*, Vol. 39, pp. 217～237.

Green, A. E. and Rivlin, R. S., 1956, "Steady Flow of Non-Newtonian Fluids through Tubes," *Q. Appl. Math.*, Vol. 14, pp. 299～308.

Hartnett, J. P. and Kostic, M., 1985, "Heat Transfer to a Viscoelastic Fluid in Laminar Flow through a Rectangular Channel," *Int. J. Heat and Mass Transfer*, Vol. 28, pp. 1147～1155.

Hartnett, J. P., 1991, *Viscoelastic Fluids : Experimental Challenges, Experimental Heat Transfer, Fluid Mechanics, Thermodynamics*, Elsevier Science Publishing Company, pp. 621～626.

Hayase, T., Humphrey, J. A. C. and Greif, R., 1992, "A Consistently Formulated QUICK Scheme for Fast and Stable Convergence Using Finite-Volume Iterative Calculation Procedures," *J. Computational Physics*, Vol. 98, pp. 108～118.

Kim, B. S., Shin, S. and Sohn, C. H., 1997, "Numerical Heat Transfer in a Rectangular Duct with a Non-Newtonian Fluid with Shear-rate Dependent Thermal Conductivity," *Trans. KSME B in Korea*, Vol. 21(6), pp. 773～778.

Kostic, M., 1994, "On Turbulent Drag and Heat Transfer Reduction Phenomena and Laminar Heat Transfer Enhancement in Non-circular Duct Flow of Certain Non-Newtonian Fluids," *Int. J. Heat Mass transfer*, Vol. 37, No. 1, pp. 133～147.

Rohsenow, W. M., Hartnett, J. P. and Cho, Y. I., 1998, *Handbook of Heat Transfer*, McGraw-Hill, New York, pp. 10.1～10.53

Shin, S. and Cho, Y. I., 1994, "Laminar Heat Transfer in a Rectangular Duct with a Non-Newtonian Fluid with Temperature Dependent Viscosity," *Int. J. Heat and Mass Transfer*, Vol. 37, pp. 19～30.

Shin, S., Ahn, H. H., Cho, Y. I. and Sohn, C. H., 1999, "Heat Transfer Behavior of a Temperature-Dependent Non-Newtonian Fluids with Reiner-Rivlin Model in a 2:1 Rectangular Ducts," *Int.l J. Heat and Mass Transfer*, Vol. 42, pp. 2935～2942.

Sohn, C. H., Ahn, S. T. and Shin, S., 2000,

"Heat Transfer Behavior of Temperature-Dependent Viscoelastic Non-Newtonian Fluid with Buoyancy Effect in 2:1 Rectangular Duct," *Int. Comm. Heat Mass Transfer*, Vol. 27, pp. 159~168.

Xie, Chunbo and Hartnett, J. P., 1992, "Influence of Rheology on Laminar Heat Tranfer to Viscoelastic Fluids in a Rectangular Channel," *Ind. Engng Chem. Res*, Vol. 31, pp. 727~732.